Inorg. Chem. **2008**, *47*, 9111−9120

Insertion of a Spin Crossover Fe^{III} Complex into an Oxalate-Based Layered Material: Coexistence of Spin Canting and Spin Crossover in a Hybrid Magnet

Miguel Clemente-León,*,†,⊥ Eugeno Coronado,*,† M. Carmen Giménez-López,† Alejandra Soriano-Portillo,† João C. Waerenborgh,‡ Fernando S. Delgado,§ and Catalina Ruiz-Pérez∥

Instituto de Ciencia Molecular, Universidad de Valencia, Polígono de la Coma s/n, 46980 Paterna, Spain, Dept. Quimica, Instituto Tecnológico e Nuclear/CFMC-UL, P-2686-953 Sacavém, Portugal, LLS-BM16 European Synchrotron Radiation Facility, 6 Rue Jules Horowitz − BP 220, 38043 Grenoble, CEDEX 9, France, Laboratorio de Rayos X y Materiales Moleculares, Departamento de Física Fundamental II, Facultad de Física de la Universidad de La Laguna, Avda. Francisco Sánchez s/n, 38024 La Laguna, Tenerife, Spain

Received June 24, 2008

The syntheses, structures, and magnetic properties of the compounds of formula $[Fe^{III}(sal_2trien)]_2[Mn^{II}_2(ox)_3]\cdot 4H_2O\cdot C_3H_7NO$ (**1**) and $[In^{III}(sal_2trien)]_2[Mn^{II}_2(ox)_3]\cdot 3H_2O\cdot CH_3OH$ (**2**) are reported. The structure presents a homometallic 2D honeycomb anionic layer formed by Mn^{II} ions linked through oxalate ligands and a cationic double layer of $[Fe(sal_2trien)]^+$ or $[In(sal_2trien)]^+$ complexes intercalated between the 2D oxalate network. The magnetic properties and Mössbauer spectroscopy of **1** indicate the coexistence of a magnetic ordering of the Mn(II) oxalate network that behaves as a weak ferromagnet and a gradual spin crossover of the intercalated $[Fe(sal_2trien)]^+$ complexes.

Introduction

One of the hot topics in molecular magnetism deals with the search of molecule-based magnets exhibiting multifunctionality. The simplest case of this kind is that provided by dual-function materials in which two properties coexist in the same crystal structure. A suitable approach to obtain such materials is the so-called hybrid approach in which two-network solids are constructed via self-assembling of two different molecular fragments (organic, inorganic, or organometallic), with each network furnishing distinct physical/structural properties to the solid.[1]

Bimetallic oxalate-bridged complexes of formula $A[M^{II}M^{III}(ox)_3]$ (M^{III} = Cr, Fe, Ru, V, Mn; M^{II} = Mn, Fe, Co, Ni, Cu, Zn) have provided many examples of hybrid magnets. These bimetallic salts are composed by a polymeric 2D honeycomb-like anionic network, which furnishes the cooperative magnetic properties (ferro-, ferri-, or canted antiferromagnetism),[2] and a bulky charge-compensating molecular cation, which controls the network formation and determines the interlayer separation. When this templating cation is also electroactive, a hybrid magnet in which the cooperative magnetism can coexist with the electronic property provided by the cationic molecular lattice can be obtained. Some illustrative examples of this concept are provided by the use of paramagnetic decamethylferrocenium cations,[3] photochromic molecules,[4,5] nonlinear-optical-active molecules,[6] and organic π-electron donors,[7−9] which lead to the formation of magnetic multilayers, photochromic

* Author to whom correspondence should be addressed. Phone: (+34) 96 3544415. Fax: (+34) 96 354 3273. E-mail: miguel.clemente@uv.es (M.C.-L.); eugenio.Coronado@uv.es (E.C.).
† Universidad de Valencia.
‡ Instituto Tecnológico e Nuclear/CFMC-UL.
§ LLS-BM16 European Synchrotron Radiation Facility.
∥ Universidad de La Laguna.
⊥ Fundació General de la Universitat de València (FGUV).

(1) (a) Coronado, E.; Day, P. *Chem. Rev.* **2004**, *104*, 5419. (b) Coronado, E.; Galán-Mascarós, J. R. *J. Mater. Chem.* **2005**, *15*, 66.

(2) (a) Tamaki, H.; Zhong, Z. J.; Matsumoto, N.; Kida, S.; Koikawa, M.; Achiwa, N.; Hashimoto, Y.; Okawa, H. *J. Am. Chem. Soc.* **1992**, *114*, 6974. (b) Tamaki, H.; Mitsumi, M.; Nakamura, N.; Matsumoto, N.; Kida, S.; Okawa, H.; Ijima, S. *Chem. Lett.* **1992**, 1975. (c) Mathonière, C.; Carling, S. G.; Yuscheng, D.; Day, P. *J. Chem. Soc., Chem. Commun.* **1994**, 1551. (d) Mathonière, C.; Nutall, J.; Carling, S. G.; Day, P. *Inorg. Chem.* **1996**, *35*, 1201. (e) Pellaux, R.; Schmalle, H. W.; Huber, R.; Fisher, P.; Hauss, T.; Ouladdiaf, B.; Decurtins, S. *Inorg. Chem.* **1997**, *36*, 2301. (f) Coronado, E.; Galán-Mascarós, J. R.; Gómez-García, C. J.; Martínez-Agudo, J. M.; Martínez-Ferrero, E.; Waerenborgh, J. C.; Almeida, M. *J. Solid State Chem.* **2001**, *159*, 391. (g) Min, K. S.; Rhinegold, A. L.; Miller, J. S. *Inorg. Chem.* **2005**, *44*, 8433. (h) Coronado, E.; Galán-Mascarós, J. R.; Martí-Gastaldo, C. *J. Mat. Chem.* **2006**, *16*, 2685.

10.1021/ic801165b CCC: $40.75
Published on Web 09/10/2008

magnets, or ferromagnetic molecular metals, respectively. Notice that, depending on the nature of the templating cation (size, shape, and charge), other magnetic networks, different from the 2D honeycomb-like network, can also be obtained with dimensionalities ranging from 0D to 3D.[10] The most extensive one is represented by the family of 3D chiral structures in which the chirality of a templating cation of the type $[Z^{II}(bpy)_3]^{2+}$ (Z^{II} = Fe, Co, Ni, Ru) induces the building blocks to adopt a homochiral configuration.[11] The hybrid character of these series also leads to examples in which the two sublattices are magnetic. Still, the chiral character of the 3D bimetallic oxalate framework is the most interesting feature of this family, as it provides the opportunity to obtain chiral magnets.[11e,12]

Owing to the structural versatility exhibited by these oxalate-based magnets, it seemed to us of interest to use a spin-crossover Fe^{III} complex as a templating cation. In the spin-crossover complexes, the transition between the low-spin (LS) and the high-spin (HS) states is triggered by a given external perturbation (light irradiation, pressure or temperature change), and the response (change of the optical and magnetic properties) may be observed abruptly with a hysteretic behavior in the solid state. This switching behavior is accompanied by a change in the size of the spin-crossover complex. Thus, an attractive possibility is to incorporate the spin-crossover complex into a molecule-based magnet with the aim of obtaining a hybrid magnet in which the critical temperature of the magnet can be tuned by applying an external stimulus (light, pressure) acting on the spin-crossover component.

In this work, we show that the spin-crossover monocation $[Fe(sal_2trien)]^+$ can be combined with oxalate-based magnets in order to obtain hybrid magnets with a coexistence of long-range magnetic ordering and spin crossover. Notice that this complex and its derivatives have already been intercalated within an amorphous $MnPS_3$ layered magnet[13] and combined with the dithiolene aceptor, $[Ni(dmit)_2]^-$.[14,15] In the first case, a thermal spin-crossover of the guest molecule and a ferromagnetic ordering of the host lattice were observed. Furthermore, a spin polarization effect on the LS Fe^{III} intercalated complex was observed below the ordering temperature by Mössbauer spectroscopy.[13a] In the second case, a cooperative spin transition of the Fe^{III} complex was obtained in contrast to other $[Fe(sal_2trien)]^+$ salts reported in the literature.[14] On the other hand, some initial attempts to combine spin-crossover complexes with extended oxalate magnetic lattices in crystalline compounds were reported in the past. Thus, Decurtins et al.[16] reported the occurrence of spin-crossover in a $[Co^{II}(bpy)_3]^{2+}$ complex inserted into the 3D oxalate-based network $[LiCr(ox)_3]^{2-}$. Still, in this bimetallic lattice, the Cr^{3+} ions were separated by diamagnetic Li^+ ions, and hence, no long-range magnetic ordering was observed. More recently, we have reported an example in which a Fe^{II} spin-crossover complex, $[Fe^{II}bpp_2]^{2+}$, is inserted in a ferromagnetic 3D oxalate-based network.[17] This compound presents a ferromagnetic ordering below 3 K, but the occurrence of spin-crossover is not observed.

Here, we report the syntheses and the structural and magnetic characterization of the compounds of formulas $[Fe^{III}(sal_2trien)]_2[Mn^{II}_2(ox)_3]\cdot 4H_2O\cdot C_3H_7NO$ (**1**) and $[In^{III}(sal_2trien)]_2[Mn^{II}_2(ox)_3]\cdot 3H_2O\cdot CH_3OH$ (**2**).

Experimental Section

Synthesis. The complexes $[Fe(sal_2trien)]PF_6$ and $[In(sal_2trien)]PF_6$ were prepared according to literature methods.[18] $Ag_3[Cr(ox)_3]$ was prepared by metathesis from the corresponding potassium salt.[19] All other materials and solvents were commercially available and used without further purification.

$[Fe(sal_2trien)]_2[Mn_2(ox)_3]\cdot 4H_2O\cdot C_3H_7NO$ (1) and $[In(sal_2trien)]_2[Mn_2(ox)_3]\cdot 3H_2O\cdot CH_3OH$ (2). A total of 0.134 g (0.67 mmol) of $MnCl_2\cdot 4H_2O$ was added to a suspension of $Ag_3[Cr(ox)_3]$ (0.288 g, 0.45 mmol) in 25 mL of methanol. The AgCl precipitate was filtered, and then the clear solution was added dropwise to a solution of $[M(sal_2trien)]PF_6$ (M = Fe, In; 0.45 mmol) in 75 mL of methanol. After refluxing the mixture for 1 h, a brown (M = Fe) or yellow (M = In) precipitate was obtained and collected by filtration. Single crystals of **1** and **2** were obtained by dissolving this precipitate in dimethylformamide and layering with methanol. Brown platelike crystals of **1** and yellow platelike single crystals of **2** were obtained

(3) (a) Coronado, E.; Galán-Mascarós, J. R.; Gómez-García, C. J.; Ensling, J.; Gutlich, P. *Chem.—Eur. J.* **2000**, *6*, 552. (b) Coronado, E.; Galán-Mascarós, J. R.; Gómez-García, C. J.; Martínez-Agudo, J. M. *Adv. Mater.* **1999**, *11*, 558. (c) Clemente-León, M.; Galán-Mascarós, J. R.; Gómez-García, C. J. *Chem. Commun.* **1997**, 1727.

(4) Bénard, S.; Yu, P.; Audière, J. P.; Rivière, E.; Clèment, R.; Ghilhem, J.; Tchertanov, L.; Nakatami, K. *J. Am. Chem. Soc.* **2000**, *122*, 9444.

(5) Aldoshin, S. M.; Sanina, N. A.; Minkin, V. I.; Voloshin, N. A.; Ikorskii, V. N.; Ovcharenko, V. I.; Smirnov, V. A.; Nagaeva, N. K. *J. Mol. Struct.* **2007**, *826*, 69.

(6) Bénard, S.; Rivière, E.; Yu, P.; Nakatami, K.; Delouis, J. F. *Chem. Mater.* **2001**, *13*, 159.

(7) Coronado, E.; Galán-Mascarós, J. R.; Gómez-García, C. J.; Laukhin, V. *Nature* **2000**, *408*, 447.

(8) Alberola, A.; Coronado, E.; Galán-Mascarós, J. R.; Giménez-Saiz, C.; Gómez-García, C. J. *J. Am. Chem. Soc.* **2003**, *125*, 10774.

(9) Coronado, E.; Galán-Mascarós, J. R.; Gómez-García, C. J.; Martínez-Ferrero, E.; Van Smaalen, S. *Inorg. Chem.* **2004**, *43*, 4808.

(10) (a) Rochon, F. D.; Melanson, R.; Andruh, M. *Inorg. Chem.* **1996**, *35*, 6086. (b) Andruh, M.; Melanson, R.; Stager, C. V.; Rochon, F. D. *Inorg. Chim. Acta* **1996**, 309. (c) Stanica, N.; Stager, C. V.; Cimpoesu, M.; Andruh, M. *Polyhedron* **1998**, *17*, 1787. (d) Marinescu, G.; Andruh, M.; Lescouëzec, R.; Muñoz, M. C.; Cano, J.; Lloret, F.; Julve, M. *New J. Chem.* **2000**, *24*, 527. (e) Triki, S.; Berezovsky, F.; Pala, J. S.; Coronado, E.; Gómez-García, C. J.; Clemente, J. M.; Riou, A.; Molinie, P. *Inorg. Chem.* **2000**, *39*, 3771. (f) Ballester, G.; Coronado, E.; Giménez-Saiz, C.; Romero, F. M. *Angew. Chem., Int. Ed.* **2001**, *40*, 792. (g) Coronado, E.; Giménez-Saiz, C.; Galán-Mascarós, J. R.; Gómez-García, C. J.; Ruiz-Pérez, C. *Eur. J. Inorg. Chem.* **2003**, 2290. (h) Coronado, E.; Galán-Mascarós, J. R.; Gómez-García, C. J.; Martí-Gastaldo, C. *Inorg. Chem.* **2005**, *44*, 6179. (i) Coronado, E.; Galán-Mascarós, J. R.; Martí-Gastaldo, C. *Inorg. Chem.* **2006**, *45*, 1882. (j) Coronado, E.; Galán-Mascarós, J. R.; Martí-Gastaldo, C.; Murcia-Martínez, A. *Dalton Trans.* **2006**, 3294. (k) Kou, H. Z.; Sato, O. *Inorg. Chem.* **2007**, *46*, 9513. (l) Cariati, E.; Macchi, R.; Roberto, D.; Ugo, R.; Galli, S.; Casati, N.; Macchi, P.; Sironi, A.; Bogani, L.; Caneschi, A.; Gatteschi, D. *J. Am. Chem. Soc.* **2007**, *129*, 9410. (m) Clemente-León, M.; Coronado, E.; Dias, J. C.; Soriano-Portillo, A.; Willett, R. D. *Inorg. Chem.* **2008**, *47*, 6458.

(11) (a) Decurtins, S.; Schmalle, H. W.; Schneuwly, P.; Oswald, H. R. *Inorg. Chem.* **1993**, *32*, 1888. (b) Decurtins, S.; Schmalle, H. W.; Schneuwly, P.; Ensling, J.; Gütlich, P. *J. Am. Chem. Soc.* **1994**, *116*, 9521. (c) Hernández-Molina, M.; Lloret, F.; Ruiz-Pérez, C.; Julve, M. *Inorg. Chem.* **1998**, *37*, 4141. (d) Coronado, E.; Galán-Mascarós, J. R.; Gómez-García, C. J.; Martínez-Agudo, J. M. *Inorg. Chem.* **2001**, *40*, 113. (e) Pointillart, F.; Train, C.; Gruselle, M.; Villain, F.; Schmalle, H. W.; Talbot, D.; Gredin, P.; Decurtins, S.; Verdaguer, M. *Chem. Mater.* **2004**, *16*, 832. (f) Clemente-León, M.; Coronado, E.; Gómez-García, C. J.; Soriano-Portillo, A. *Inorg. Chem.* **2006**, *45*, 5653.

(12) (a) Andrés, R.; Gruselle, M.; Malézieux, B.; Verdaguer, M.; Vaissermann, J. *Inorg. Chem.* **1999**, *38*, 4637. (b) Andrés, R.; Brissard, M.; Gruselle, M.; Train, C.; Vaissermann, J.; Malézieux, B.; Jamet, J. P.; Verdaguer, M. *Inorg. Chem.* **2001**, *40*, 4633.

Table 1. Crystal Data and Structure Refinement Details for $[Fe(sal_2trien)]_2[Mn_2(ox)_3]\cdot 4H_2O\cdot C_3H_7NO$ (**1**) and $[In(sal_2trien)]_2[Mn_2(ox)_3]\cdot 3H_2O\cdot CH_3OH$ (**2**)

compound	**1**	**2**
empirical formula	$C_{49}H_{63}Fe_2Mn_2N_9O_{21}$	$C_{47}H_{48}In_2Mn_2N_8O_{20}$
fw	1335.66	1383.98
temperature (K)	100(2)	180(1)
wavelength (Å)	0.7293	0.71073
cryst syst	monoclinic	monoclinic
space group	$P2_1/c$	$P2_1/c$
a (Å)	10.287(2)	17.3940(3)
b (Å)	15.608(3)	15.3870(6)
c (Å)	34.978(7)	10.3820(6)
α (deg)	90	90
β (deg)	97.82(3)	97.2960(18)
γ (deg)	90	90
Z	4	4
ρ_{calc} (Mg/cm^3)	1.595	1.668
cryst size (mm)	0.098 × 0.080 × 0.026	0.120 × 0.090 × 0.030
V (Å^3)	5563.9(9)	2756.2(2)
θ range of data collection (deg)	1.47−21.84	1.77−24.15
refln collection/unique	35396/5626	8198/4398
refinement method	full-matrix least-squares on F^2	full-matrix least-squares on F^2
data/restraints/parameters	5626/ 2 /771	4398/0/379
goodness-of-fit on F2	1.062	1.174
final R indices [$I > 2\sigma(I)$]	$R_1 = 0.0887$, $R_W^2 = 0.2464$	$R_1 = 0.0553$, $R_W^2 = 0.1515$

after 1 month. The composition of these crystals was checked by microanalysis. These measurements showed that the M/Mn (M = Fe or In) ratio is 1:1.

Structural Characterization. Crystal data and other details of the structure analyses are presented in Table 1. A single crystal of **1** was mounted and X-ray diffraction data were collected at 100 K on the Spanish CRG-BM16 beamline at the ESRF using synchrotron radiation (λ = 0.7293 Å) and an ADSC Q210r detector. Single crystals of **2** were mounted and collected on a nonius KappaCCD diffractometer equipped with graphite-monochromated Mo Kα radiation (λ = 0.71073 Å). X-ray diffraction data for **2** were collected at 180 K. The Denzo and Scalepack programs were used for cell refinements and data reduction of both compounds.[20] The structure of **1** was solved by direct methods using the SHELXS-97[21] program, while the structure of **2** was solved by direct methods using the SIR97 program.[22] Both structures were refined on F^2 with the SHELXL-97 program.[21] In the two structures, hydrogen atoms were added in calculated positions and refined riding on the corresponding atoms.

Physical Measurements. Magnetic susceptibility measurements were performed on polycrystalline samples using a magnetometer (Quantum Design MPMS-XL-5) equipped with a SQUID sensor. Variable-temperature measurements were carried out in the temperature range 2−400 K. The ac measurements were performed in the temperature range 2−10 K at different frequencies with an oscillating magnetic field of 0.395 mT. The magnetization and hysteresis studies were performed between +5 and −5 T, cooling the samples at zero field. The Fe/Mn/Cr and In/Mn/Cr ratios were measured on a Philips ESEM X230 scanning electron microscope equipped with an EDAX DX-4 microsonde. Mössbauer spectra were collected in transmission mode using a conventional constant-acceleration spectrometer and a 25 mCi ^{57}Co source in a Rh matrix. The velocity scale was calibrated using α-Fe foil. The absorber was obtained by pressing powdered single crystals of **1** into a perspex holder. Low-temperature spectra were collected using a bath cryostat with the sample immersed in liquid He, for measurements at 4.1 K, or by using flowing He gas to cool the sample above 4.1 K (temperature stability of 0.2 K). The spectra were fitted to Lorentzian lines using a nonlinear least-squares method.[23] Isomer shifts (Table 2) are given relative to metallic α-Fe at room temperature.

Table 2. Estimated Parameters from the Mössbauer Spectra of **1** Taken at Different Temperatures[a]

		IS	QS	B_{hf}	Γ	I
297 K	HS Fe	0.14	0.55		0.32	100%
160 K	LS Fe	0.16	2.64		0.59	26%
	HS Fe	0.22	0.56		0.62	74%
80 K	LS Fe	0.20	2.73		0.46	52%
	HS Fe	0.27	0.56		0.60	48%
4.5 K	LS Fe	0.21	2.93		0.51	53%
	HS Fe	0.27	0.59		0.45	35%
	HS Fe(ox)	0.49	0.09	52.6	0.38	12%

[a] HS Fe and LS Fe: high-spin and low-spin Fe^{III} in $[Fe(sal_2trien)]^+$. Fe(ox): high-spin Fe^{III} in the oxalate layers. IS (mm/s): isomer shift relative to metallic Fe at 297 K. QS (mm/s): quadrupole splitting of doublets; ε (mm/s), quadrupole shift for magnetic sextet. B_{hf} (T): magnetic hyperfine field. Γ (mm/s): half-width of the doublet peaks. I: relative area. Estimated standard deviations are <0.02 mm/s for IS, QS, ε, and Γ, < 0.5 T for B_{hf}, and <2% for I.

Results and Discussion

Synthesis and Structure. The Fe^{III} spin-crossover complex, $[Fe(sal_2trien)]^+$, and its diamagnetic analogue, $[In(sal_2trien)]^+$, which has been used as a reference to

(13) (a) Floquet, S.; Salunke, S.; Boillot, M.-L.; Clément, R.; Varret, F.; Boukheddaden, K.; Rivière, E. *Chem. Mater.* **2002**, *14*, 4164–4171. (b) Floquet, S.; Muñoz, M. C.; Rivière, E.; Clément, R.; Audière, J. P.; Boillot, M. L. *New J. Chem.* **2004**, *28*, 535.

(14) Dorbes, S.; Valade, L.; Real, J. A.; Faulmann, C. *Chem. Commun.* **2005**, *69*.

(15) Faulmann, C.; Dorbes, S.; Real, J. A.; Valade, L. *J. Low Temp. Phys.* **2006**, *142*, 261.

(16) Sieber, R.; Decurtins, S.; Stoeckli-Evans, H.; Wilson, C.; Yufit, D.; Howard, J. A. K.; Capelli, S. C.; Hauser, A. *Chem.−Eur. J.* **2000**, *6*, 361.

(17) Coronado, E.; Galán-Mascarós, J. R.; Giménez-López, M. C.; Almeida, M.; Waerenborgh, J. C. *Polyhedron* **2007**, *26*, 1838.

(18) Sinn, E.; Sim, G.; Dose, E. V.; Tweedle, M. F.; Wilson, L. J. *J. Am. Chem. Soc.* **1978**, *100*, 3375.

(19) Baylar, J. C.; Jones, E. M. In *Inorganic Synthesis*; Booth, H. S. Ed.; McGraw-Hill: New York, 1939; Vol. 1, p 35.

(20) Otwinowski, Z.; Minor, W. *In Methods in Enzymology*, Carter, C. W., Jr.; Sweet, R. M. Eds.; Academic Press: New York, 1997; Vol. 276, p 307.

(21) Sheldrick, G. M. *SHELX-97*, release 97-2; Institüt für Anorganische Chemie der Universität: Göttingen, Germany, 1998.

(22) Altomare, A.; Burla, M. C.; Camalli, M.; Cascarano, G. L.; Giacovazzo, C.; Guagliardi, A.; Moliterni, A. G. G.; Polidori, G.; Spagna, R. *J. Appl. Crystallogr.* **1999**, *32*, 115.

(23) Waerenborgh, J. C.; Figueiredo, M. O.; Cabral, J. M. P.; Pereira, L.C. J. *J. Solid State Chem.* **1994**, *111*, 300.

understand the properties of the Fe^{III} analogue, have been added to a methanolic solution containing $[Cr^{III}(ox)_3]^{3-}$ and Mn^{2+}. $Ag_3[Cr(ox)_3]$ was used as the $[Cr^{III}(ox)_3]^{3-}$ source to avoid the presence of alkali ions in the structure. Thus, this Ag^+ salt reacted with the $MnCl_2 \cdot 4H_2O$ salt to give rise to a precipitate of AgCl and to a clear solution containing solely the ions $[Cr^{III}(ox)_3]^{3-}$ and Mn^{2+} in a ratio of 2:3. This solution was then mixed and refluxed over 1 h with a solution containing the $[M(sal_2trien)]^+$ complex. The resulting brown (M = Fe) and yellow (M = In) precipitates were analyzed with a scanning electron microscope equipped with an EDAX microsonde. The results indicate that Mn, Cr, and M are in a 1:1:1 ratio. The preparation of good crystals of these compounds by slow diffusion was not possible. As these precipitates were partially soluble in dimethylformamide, a layering with methanol was carried out. This resulted in the formation of brown crystals of **1** and violet crystals of **2** after a few weeks. The structure of these crystals was solved by single-crystal X-ray diffraction. Analysis of these compounds indicated a change in the chemical composition with respect to the initial precipitate. Thus, Cr metal is not present in the final crystals, but only in the other two that are present in a 1:1 ratio. From the single-crystal X-ray diffraction studies, the formulas of the two compounds are $[Fe(sal_2trien)]_2[Mn_2(ox)_3] \cdot 4H_2O \cdot C_3H_7NO$ (**1**) and $[In(sal_2trien)]_2[Mn_2(ox)_3] \cdot 3H_2O \cdot CH_3OH$ (**2**).

A possible mechanism that may explain the formation of the homometallic $[Mn_2(ox)_3]^{2-}$ anion lattice is the slow decomposition of the $[Cr(ox)_3]^{3-}$ complexes of the initial precipitate after being dissolved in dimethylformamide. The free oxalate ligands resulting from the partial decomposition of $[Cr(ox)_3]^{3-}$ could coordinate to the solvated Mn^{2+} ions leading to the formation of a new 2D extended network formed by Mn^{2+} ions linked through the oxalate ligands. This anionic network precipitates in the presence of the $[M(sal_2trien)]^+$ cation giving rise to the crystallization of **1** and **2**. Attempts to obtain a similar product without using the $[Cr(ox)_3]^{3-}$ complex were not successful. Therefore, it seems that the slow decomposition of the quite inert $[Cr(ox)_3]^{3-}$ complex in dimethylformamide/MeOH is the crucial point that enables the slow precipitation of these compounds as good crystals. The use of other M^{II} ions such as Ni, Co, or Fe or other more labile oxalate complexes such as $[Fe(ox)_3]^{3-}$ did not lead to the formation of analogous derivatives.

The structure of $[Fe(sal_2trien)]_2[Mn_2(ox)_3] \cdot 4H_2O \cdot C_3H_7NO$ (**1**) is formed by anionic sheets in the *ab* plane of formula $[Mn_2(ox)_3]^{2-}$ with interlamellar $[Fe(sal_2trien)]^+$, water, methanol, and dimethylformamide molecules (Figure 1a). The anionic layer is formed by an extended network with Mn^{2+} ions linked through oxalate bridges. The extended oxalate network resembles a 2D honeycomb structure. It is formed by oxalate ligands connecting two crystallographically independent Mn^{II} ions (Mn(1,2)) in such a way that each Mn(1) is surrounded by three neighboring Mn(2)'s (Figure 2a). These layers are stacked one over the other in an *ABAB*... fashion. The mean Mn−O distances ranges between 2.136(6) and 2.208(6) Å for Mn(1) and between 2.140(7) and 2.191(6) Å for Mn(2). These values support the presence of Mn^{II} ions in the 2D layer since they are typical Mn^{II}−O distances. Thus, the 3D Mn−oxalate network of the $[Ru(bpy)_3][Mn_2(ox)_3]$ compound presents very similar Mn−O distances of 2.133 and 2.168 Å.[24] The main novelty of this structure is that this homometallic network exhibits a 2D honeycomb structure, which is the structure typically associated with the bimetallic $M^{II}M^{III}$ networks. The other known 2D homometallic honeycomb structures are two Zn oxalates of formulas $[(CH_3)_2NH(CH_2)_3NH_3][Zn_2(ox)_3].2H_2O$[25] and $K[C_6N_2H_{13}][Zn_2(ox)_3] \cdot 4H_2O$,[26] obtained by hydrothermal synthesis. Still, this is the first example of a homometallic oxalate-based 2D structure in which the metal ions are paramagnetic. All of the other homometallic Mn^{II}−oxalate networks reported in the literature exhibit the typical 3D chiral lattice. These have been obtained in the hybrid salts $[Z(bpy)_3][Mn_2(ox)_3]$ (Z = Fe^{II}, Ni^{II}), where the −2 charge of the anionic layer is compensated by a chiral cation with a +2 charge.[11b,24] On the other hand, the presence of Mn^{II} ions as the only metals of this network induces a distortion of the honeycomb structure. Thus, the hexagonal rings are slightly elongated along the *a* axis (see Figure 2a). Furthermore, the Mn ions and oxalate ligands do not form a perfect 2D layer, and a certain undulation of the inorganic layer can be observed (see Figure 1a).

Another distinctive feature of this structure is the presence of a double layer of inorganic cationic complexes instead of the single cationic layer of the $M^{II}M^{III}$ honeycomb structures. The presence of an additional layer of cations is necessary to compensate the higher charge of the $[Mn_2(ox)_3]^{2-}$ anionic layer with respect to the $[M^{II}M^{III}(ox)_3]^-$ anionic layer. A consequence of this is that the interlayer distances found in this compound (Mn−Mn interlayer distance is 17.489(7) Å) are much longer than those found in the $M^{II}M^{III}$ honeycomb structures (9.2−9.7 Å in other $M^{II}M^{III}$ 2D structures[3a]).

The cationic double layer contains two crystallographically independent $[Fe(sal_2trien)]^+$ complexes, one dimethylformamide molecule, and four water molecules (Supporting Information). The two crystallographically independent $[Fe(sal_2trien)]^+$ complexes form double chains running along the *a* axis (Figure 1a). The $[Fe(sal_2trien)]^+$ complexes are connected through $\pi-\pi$ stacking interactions. Thus, each aromatic ring of sal_2trien interacts with adjacent $[Fe(sal_2trien)]^+$ complexes or dimethylformamide solvent molecules. In the case of the two phenolato rings of Fe(1), there are two types of $\pi-\pi$ stacking interactions. One of the two phenolato rings presents very short distances with one dimethylformamide molecule ($d_{C25-C61}$ = 3.553 Å, $d_{C27-N61}$ = 3.317 Å), while the second one interacts through $\pi-\pi$ stacking interactions with an adjacent phenolato ring of Fe(2) ($d_{C38-C47}$ = 3.271 Å, $d_{C39-C47}$ = 3.308 Å) belonging to the same chain. On the other hand, the two phenolato rings

(24) Pointillart, F.; Train, C.; Boubekeur, K.; Gruselle, M.; Verdaguer, M. *Tetrahedron: Asymmetry* **2006**, *17*, 1937.
(25) Natarajan, S. *Solid State Sci.* **2002**, *4*, 1331.
(26) Vaidhyanathan, R.; Natarajan, S.; Rao, C. N. R. *Solid State Sci.* **2002**, *4*, 633.

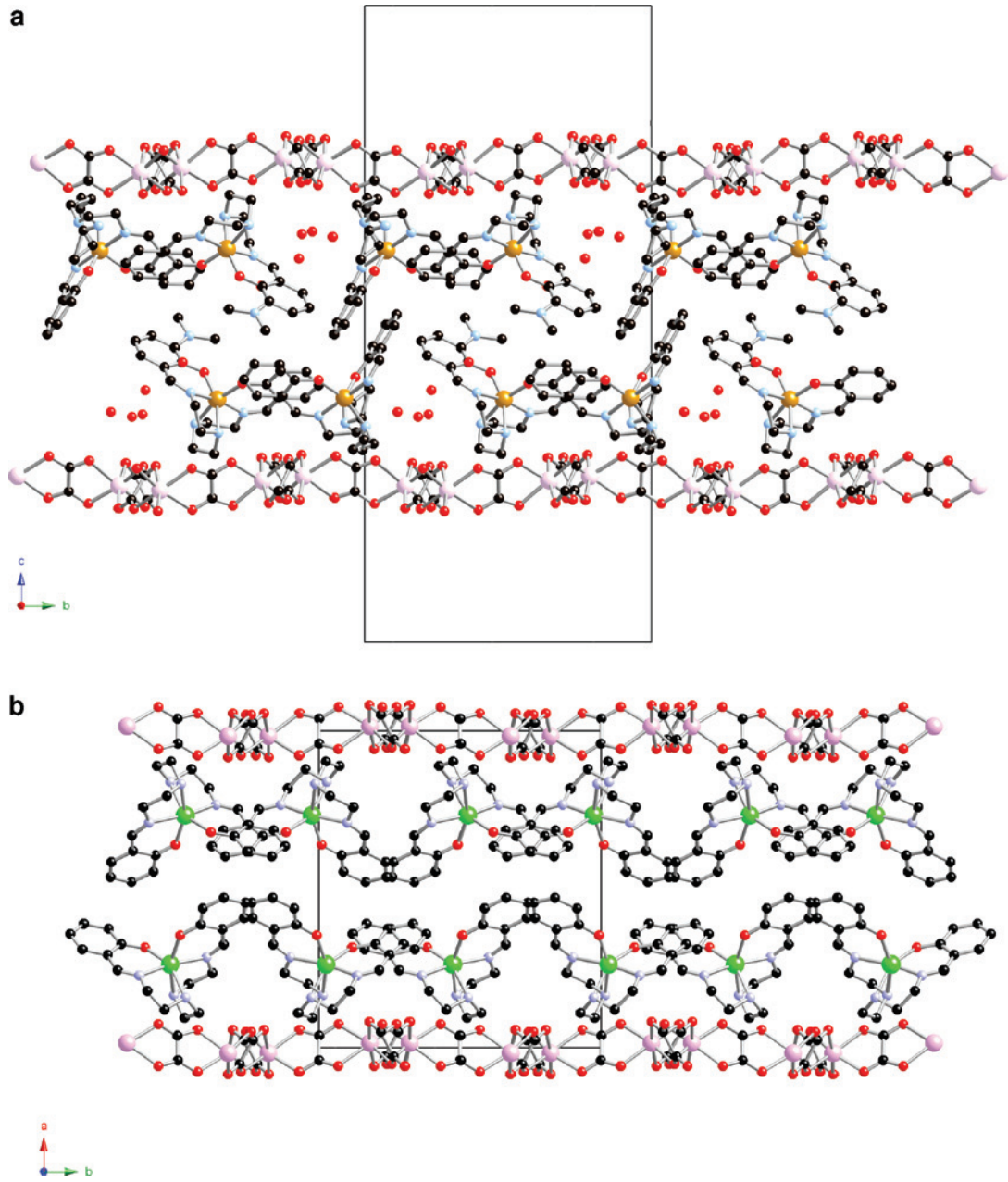

Figure 1. Projection on the *bc* plane of the structure of **1** (a). Projection on the *ab* plane of the structure of **2** (solvent molecules have been omitted for clarity). Fe (yellow), In (green), Mn (pink), C (black), N (blue), O (red).

of Fe(2) present $\pi-\pi$ stacking interactions with one phenolato ring of the adjacent Fe(1) of the same chain (see above) and with one phenolato ring of Fe(2) ($d_{C54-C56}$ = 3.315 Å) belonging to the neighboring chain. The average Fe−N and Fe−O bond distances are 2.115(8) and 1.909(7) Å for Fe(1) and 2.072(9) and 1.906(8) Å for Fe(2), respectively. These values are in the range of those obtained for other high-spin $[Fe(sal_2trien)]^+$ cations.[27] We should note that Mössbauer spectroscopy (see below) indicates that 74% of Fe is HS at 160 K and that the temperature of the structural resolution was 120 K.

The water molecules occupy the holes situated between the $[Fe(sal_2trien)]^+$ cations and the oxalate network. They are connected through hydrogen-bond interactions. Thus, O1W forms hydrogen bonds with O2W, O4W, one oxalate ligand, and one NH group from sal_2trien; O2W forms hydrogen bonds with O1W and one oxalate ligand; O3W forms hydrogen bonds with O4W and one oxalate ligand; and O4W forms hydrogen bonds with O1W and one dimethylformamide molecule.

The structure of $[In(sal_2trien)]_2[Mn_2(ox)_3]\cdot 3H_2O\cdot CH_3OH$ (**2**) resembles that of **1** with some important differences. The volume of the unit cell of **2** is halved as compared to **1**, and as a consequence, there is only one independent In(III) or Mn(II) center. Furthermore, dimethylformamide solvent molecules are not found in this structure.

The structure of **2** is formed by alternating layers of $[Mn_2(ox)_3]^{2-}$ in the *bc* plane and a double cationic layer of $[In(sal_2trien)]^+$ (Figure 1b). The anionic layers present a 2D honeycomb structure (Figure 2b) and are stacked one over the other in an *AA*... fashion in contrast to **1**, in which an *ABAB*... packing is obtained. The mean Mn−O distances

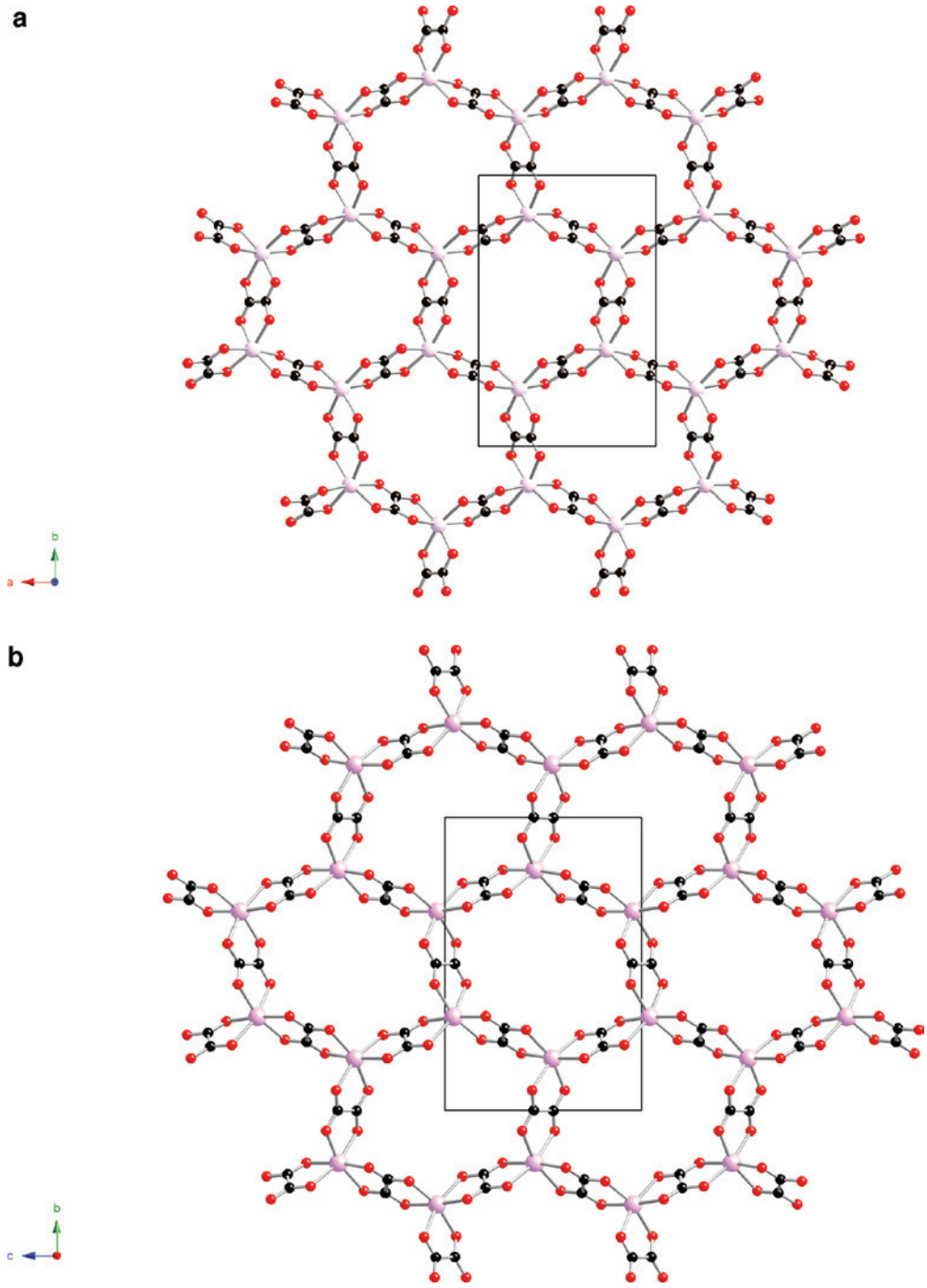

Figure 2. (a) View on the *ab* plane of the $[Mn_2(ox)_3]^{2-}$ oxalate network of **1**. (b) View on the *bc* plane of the $[Mn_2(ox)_3]^{2-}$ oxalate network of **2**.

range between 2.146(6) and 2.187(5) Å, which are close to those found for **1**. In spite of the larger diameter of $[In(sal_2trien)]^+$ compared to $[Fe(sal_2trien)]^+$, the Mn−Mn interlayer distance (17.3940(3) Å) of this compound is shorter than that of **1**. This can be explained by the more compact packing of the $[In(sal_2trien)]^+$ cations and the lack of dimethylformamide molecules.

The double layer of inorganic cationic complexes contains one crystallographically independent $[In(sal_2trien)]^+$ complex, water molecules, and methanol. The $[In(sal_2trien)]^+$ complexes are connected through $\pi-\pi$ stacking interactions, forming dimers within the same layer (Supporting Information). Thus, one of the two phenolatos of sal_2trien interacts with one phenolato ring of the adjacent $[In(sal_2trien)]^+$ complex through $\pi-\pi$ stacking interactions ($d_{C2-C7^*} = 3.236$ Å). The average In−N and In−O bond distances are 2.260(8) and 2.080(6) Å.

The disordered methanol and water solvent molecules occupy the holes between the $[In(sal_2trien)]^+$ cations and the oxalate network. The methanol molecule forms hydrogen bonds with one NH group from sal_2trien. This methanol molecule is disordered with a water molecule with an occupancy of 50%.

(27) Pritchard, R.; Barrett, S. A.; Kilner, C. A.; Halcrow, M. A. *Dalton Trans.* **2008**, 3159.

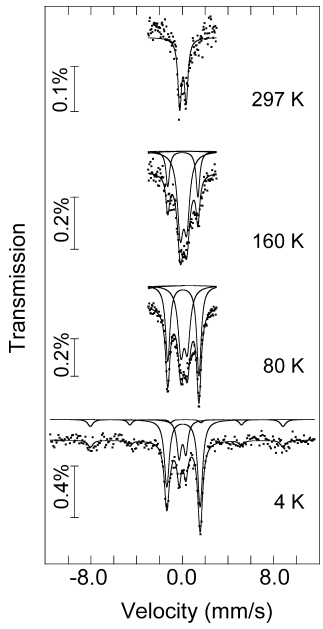

Figure 3. Mössbauer spectra of **1** taken at different temperatures. The lines over the experimental points for 160 and 80 K spectra are the sum of two doublets corresponding to HS and LS Fe^{III}. At 4 K, an additional sextet is observed. The estimated parameters for these doublets and sextet, shown slightly shifted for clarity, are collected in Table 2.

Mössbauer Spectroscopy. The room-temperature Mössbauer spectrum of the $[Fe(sal_2trien)]_2[Mn_2(ox)_3]\cdot 4H_2O\cdot C_3H_7NO$ sample, **1**, consists of a single quadrupole doublet, while spectra obtained at lower temperatures show two quadrupole doublets (Figure 3). Estimated hyperfine parameters are summarized in Table 2. The relative areas of both peaks in a quadrupole doublet are not equal very likely due to texture effects. These effects are expected since crystals used to prepare the Mössbauer absorber have a particular cleavage and the particles obtained after powdering retain a geometrical shape that should give rise to preferred orientation effects.

As usually for Fe^{III}, the doublet with the lowest quadrupole splitting, QS (Table 2), may be attributed to HS Fe^{III}, and the doublet with the highest QS to LS Fe^{III}.[13a,18,28] At 4 K, in addition to both doublets, a sextet is also observed. As discussed below this sextet is most likely due to the incorporation of a few high-spin Fe^{III} in the oxalate layers.

In contrast to LS Fe^{III}, the QS of HS Fe^{III} with $S = 5/2$, $^6A_1$, does not depend on the temperature (Table 2). For $^6A_1$, each d orbital is occupied by a single electron, and there is no electric field gradient, efg, created by the electron cloud of the Fe atom. The efg at the Fe nucleus is only due to the lattice charge distribution, and if there is no crystal structure transition in the measured temperature range, changes in QS are negligible. This is not the case with LS Fe^{III}, where the populations of the d orbital are different, creating a nonzero efg whose main component, V_{zz}, has a sign opposite that of the lattice V_{zz}. The electronic efg is however much stronger than the lattice efg, giving rise to a QS higher than that observed for $^6A_1$ Fe^{III}. Opposite signs for the electronic and the lattice V_{zz} are also consistent with texture effects being the cause for the asymmetry of the LS and HS doublets. In fact, for the LS doublet, where electronic efg predominates, the larger area is observed for the highest velocity peak, while in the HS case, where lattice efg predominates, the reverse is observed. Furthermore, low-energy excited electronic states are available for LS Fe^{III}. The electron population of these states increases with the temperature within the 4−300 K range, and consequently both the efg and the QS are strongly temperature-dependent.

The IS of the sextet observed at 4 K is significantly higher than the IS of the HS Fe^{III} doublet. On the other hand, both the high IS and magnetic hyperfine field estimated for the sextet (Table 2) are very similar to those reported for high-spin Fe^{III} in two-dimensional oxalate-bridged bimetallic complexes.[29,30] The magnetic ordering of Fe in the isolated $[Fe(sal_2trien)]^+$ cations would be surprising considering the large Fe−Fe interatomic distances. The most likely reason for the sextet appearing at 4K would be therefore the incorporation of high-spin Fe^{III} in the oxalate layers, Fe^{III}(ox). This incorporation may have occurred during the preparation procedure.[11b,30]

Mössbauer spectra therefore confirm a HS ($^6A_1$ state) to LS partial conversion of Fe^{III} in **1** as the temperature decreases down to 4 K. As a first approximation, the estimated relative areas (Table 2) may be taken as the fraction of Fe^{III} in the LS and HS states.

It should be noted that, after keeping the sample in a vacuum at room temperature for approximately 24 h, a strong broadening of the absorption peaks is observed. This broadening prevents an accurate analysis of the Mössbauer spectra in the whole 300−4 K range. It is however clear that two distributions, one of high QS contributions and another of low QS contributions, appear at 4 K. The relative area of the high QS distribution is significantly lower than the relative area of the Fe^{III} LS doublet in the 4 K spectrum of the untreated sample. This effect may be compared with that reported for the intercalation compound $[Fe(5\text{-}OMe\text{-}sal_2trien)]_{0.28}Mn_{0.86}PS_3\cdot nH_2O$ after exposure to a vacuum,[13a] when cointercalated water molecules are removed from the compound, which favors the HS state of Fe(III). The removal of solvent molecules from the present $[Fe(sal_2trien)]_2[Mn_2(ox)_3]\cdot 4H_2O\cdot C_3H_7NO$ also seems to change the stability of the Fe^{III} spin states but additionally leads to disorder in the crystal structure, as suggested by the strong broadening of the absorption lines.

Magnetic Properties. $[Fe(sal_2trien)]_2[Mn_2(ox)_3]\cdot 4H_2O\cdot C_3H_7NO$ (1). The very different magnetic behaviors of the $[Fe(sal_2trien)]^+$ salts reported in the literature[27] reveal the influence of counterion size and the associated electrostatic interactions on the spin conversion process. In the case of **1**, we will study the influence of the presence of an anionic extended network into the spin conversion process of

(28) Tweedle, M. F.; Wilson, L. J. *J. Am. Chem. Soc.* **1976**, *98*, 4824.

(29) Carling, S. G.; Visser, D.; Hautot, D.; Watts, I. D.; Day, P.; Ensling, J.; Gütlich, P.; Long, G. J. *Phys. Rev. B: Condens. Matter Mater. Phys.* **2002**, *66*, 104407.

(30) Coronado, E.; Galán-Mascarós, J. R.; Gómez-García, C. J.; Martínez-Ferrero, E.; Almeida, M.; Waerenborgh, J. C. *Eur. J. Inorg. Chem.* **2005**, *11*, 2064.

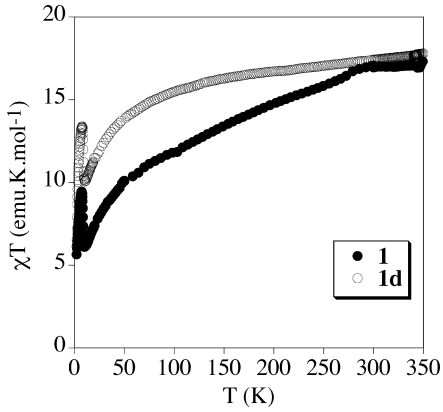

Figure 4. Temperature dependence of the product of the molar magnetic susceptibility with temperature at 0.1 T (χT) for the initial sample **1** (filled circles) and the desolvated sample **1d** (empty circles).

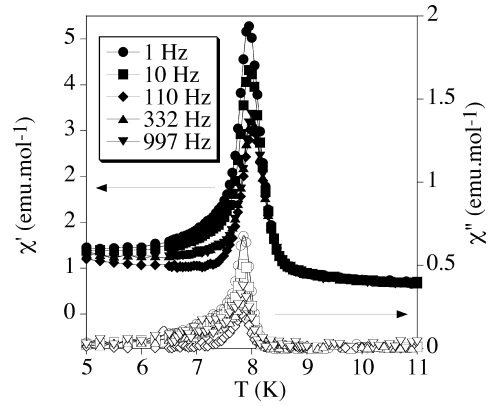

Figure 5. Temperature dependence of the in-phase AC susceptibility (χ'; filled symbols) and the out-of-phase AC susceptibility (χ''; empty symbols) for **1**.

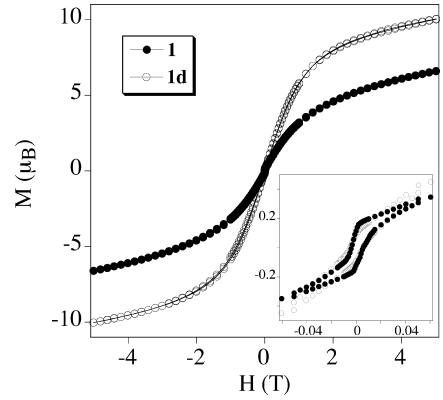

Figure 6. Field dependence of the magnetization (M) for **1** (filled circles) and **1d** (empty circles) at 2 K.

$[Fe(sal_2trien)]^+$. At the same time, we will study the influence of this spin conversion process into the magnetic properties of the extended network.

The thermal dependence of the product of the molar magnetic susceptibility with the temperature (χT) of **1** is shown in Figure 4. χT shows a constant value of 17.0 emu·K·mol^{-1} from 350 to 300 K. This value is approximately equal to the sum of the expected contributions for the isolated paramagnetic ions (two HS Fe(III) and two Mn(II)) taking into account that Mössbauer data suggest that Fe(III) is 100% HS at this temperature. χT decreases gradually from 300 to 10 K as the temperature decreases, with a more abrupt decrease below 60 K. The χT value at 80 K is 11.2 emu·K·mol^{-1}. This value of χT is again consistent with the Mössbauer data that suggest that Fe(III) is 50% LS at this temperature. Therefore, in this range of temperatures, the HS → LS spin conversion of one of the two Fe(III) centers takes place. At lower temperatures, there is a more abrupt decrease of χT to reach a minimum of 6.1 emu·K·mol^{-1} at 10 K. This behavior cannot be attributed to the spin-crossover of Fe(III) as Mössbauer data indicate that the amount of Fe(III) in the LS and the HS states remains almost constant within this temperature range. Hence, this decrease is due to the antiferromagnetic interactions between Mn(II) ions of the 2D oxalate network. The antiferromagnetic behavior of a Mn(II) oxalate network has been reported in the literature.[11b,24,31,32] Therefore, besides the HS → LS spin conversion of approximately half of the two Fe(III) centers, the antiferromagnetic interactions within the $[Mn_2(ox)_3]^{2-}$ network contribute too to the observed decrease of χT. Below 10 K, χT exhibits a sharp increase and reaches a maximum at 7.1 K with a value of 9.5 emu·K·mol^{-1}. An abrupt increase of χ is also observed at 10 K. Below this jump, χ increases continuously and does not saturate (Supporting Information). The presence of this jump below 10 K in both the χT and χ curves suggests the appearance of a magnetically ordered regime. This is confirmed by ac susceptibility measurements that show a sharp frequency-independent maximum in χ' and χ'' (Figure 5). The χ'' signal becomes nonzero at ca. 8.1 K, which defines T_c. Taking into account the nature of interacting spins of the $[Mn_2(ox)_3]^{2-}$ network, this compound can be considered to be a weak ferromagnet in which the net magnetic moment comes from canting of the antiferromagnetically aligned $S(Mn^{II}) = 5/2$ moments. A similar behavior has been observed for other Mn(II)−oxalate compounds with a 3D structure of formulas $[Fe(bpy)_3][Mn_2(ox)_3]$ and $[Ru(bpy)_3][Mn_2(ox)_3]$.[11b,24] To confirm the magnetic ordering of the spins in these compounds, isothermal magnetization at 2 K has been performed. It shows an abrupt increase at low magnetic fields and an almost linear increase at higher fields which is far from saturation at 5 T, as expected for weak ferromagnet behavior (Figure 6). A hysteresis loop of the magnetization with a coercive field of 4.8 mT also is observed.

The magnetic behavior of this compound after desolvation has been studied because removal of the solvent molecules may cause drastic changes in the spin-crossover behavior of this cation, as shown in other $[Fe(sal_2trien)]^+$ salts.[13] The sample was desolvated by heating at 400 K for 1 h. The magnetic properties of the desolvated sample, **1d**, differ notably with respect to those of **1** (see Figure 4). Complex **1d** presents higher values of χT than **1** in all of the ranges of temperatures. The difference between these two values is approximately constant and very small at temperatures above 300 K (17.5 vs 17.1 emu·K·mol^{-1} at 300 K), indicating

(31) García-Terán, J. P.; Castillo, O.; Luque, A.; García-Couceiro, U.; Beobide, G.; Román, P. *Dalton Trans.* **2006**, 902.
(32) Manna, S. C.; Zangrando, E.; Drew, M. G. B.; Ribas, J.; Chaudhuri, N. R. *Eur. J. Inorg. Chem.* **2006**, 481.

that the two Fe(III)'s of the desolvated sample are also in a HS state. The χT values of **1d** decrease more gradually at decreasing temperatures than those of **1**. Thus, χT decreases from 17.5 emu·K·mol^{-1} at 300 K to 15.0 emu·K·mol^{-1} at 80 K (11.3 emu·K·mol^{-1} for **1**). Below this temperature, χT decrease more abruptly to reach a minimum of 10.3 emu·K·mol^{-1} at 10.1 K (6.1 emu·K·mol^{-1} for **1**). Below 80 K, the χT curves of **1** and **1d** are very similar. The difference of χT values between both curves is constant and very close to 4 emu·K·mol^{-1}, which is the difference between a HS Fe(III) and a LS Fe(III). It seems, hence, that the spin-crossover is suppressed after desolvation. The decrease of χT with the temperature of **1d** is caused mainly by the antiferromagnetic coupling of the $[Mn_2(ox)_3]^{2-}$ network. This explains the similar behavior of the initial sample and the desolvated sample below 80 K, as no spin-crossover occurs within this range of temperatures in both samples. The presence of a spin conversion in the initial sample that it is suppressed in the desolvated sample can be related to the hydrogen-bonding interactions involving the N−H protons on the trien backbone of sal$_2$trien and solvent molecules that favor a LS state, as observed for other [Fesal$_2$trien]$^+$ salts.[28,33] Below 10.1 K, an abrupt increase of χT to a value of 13.4 emu·K·mol^{-1} at 7.5 K is observed. This indicates that the desolvated sample behaves also as a weak ferromagnet. Some differences appear with respect to the initial sample. Thus, both the χ' and χ'' peaks are shifted toward higher temperatures, and their intensity decreases with respect to the initial compound. The T at which χ'' is different from zero is 8.5 K for **1d** (8.1 K for **1**; Figure 7a). Hence, there is an increase of 0.4 K of the ordering temperature after desolvation (Figure 7b). Furthermore, the hysteresis loop of magnetization at 2 K is also different from that of the initial compound. The increase of magnetization with the field is more abrupt for the desolvated sample. Thus, the magnetization values of **1d**are higher than those of **1** (Figure 6). For instance, at 5 T magnetization of 10 μ_B is found for **1d** (6.6 μ_B for **1**). This is a consequence of the higher fraction of HS Fe(III) of the desolvated compound. On the other hand, the coercive field of the desolvated sample (5.3 mT) is increased with respect to that of the initial sample (4.8 mT).

This small increase in the ordering temperature after desolvation could be related to the structural changes in the 2D oxalate network induced by desolvation. Thus, the changes in angles and distances between Mn(II) ions can modify the canting between the antiferromagnetically coupled $S = 5/2$ of the Mn(II) ions, increasing slightly the ordering temperature. To know if this increase in the ordering temperature also is related to the different spin state of Fe(III) in the initial and desolvated sample, we have studied the magnetic properties after desolvation of the [Insal$_2$trien]$^+$ analogue, **2** (see below), in which no spin conversion takes place.

[In(sal$_2$trien)]$_2$[Mn$_2$(ox)$_3$]·3H$_2$O·CH$_3$OH (2). The temperature dependence of χT and χ for **2** is similar to that for

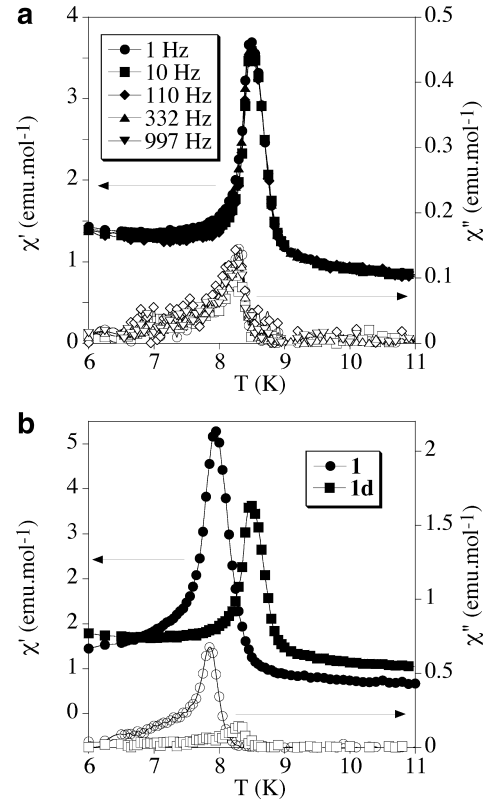

Figure 7. (a) Temperature dependence of the in-phase AC susceptibility (χ'; filled symbols) and the out-of-phase AC susceptibility (χ''; empty symbols) for the desolvated sample **1d**. (b) Temperature dependence of the in-phase AC susceptibility (χ'; filled symbols) and the out-of-phase AC susceptibility (χ''; empty symbols) at 1 Hz for **1** (circles) and **1d** (squares).

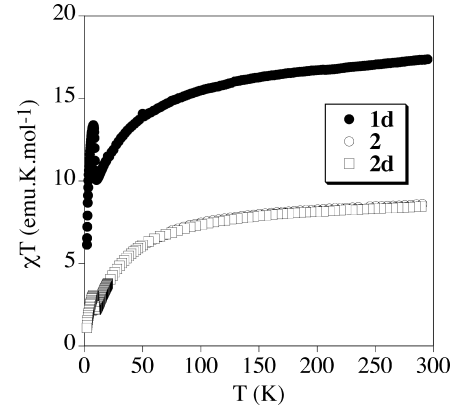

Figure 8. Temperature dependence of the product of the molar magnetic susceptibility with temperature at 0.1 T (χT) for **2** (empty circles) and the desolvated sample **2d** (empty squares) and for the desolvated **1d** (filled circles).

1d (see Figure 8 and Supporting Information). At temperatures above 12 K, the two χT curves are separated by a constant value of 8.5 emu·K·mol^{-1}, which is close to the contribution of two noninteracting HS Fe(III)'s, in agreement with the HS state of Fe(III) in **1d**. Below this temperature, there is a sharp increase of χT. The χ^{-1} versus T curve is linear in the 50−300 K temperature range. It can be fitted to a Curie−Weiss law ($\chi^{-1} = (T - \theta)/C$), leading to a Weiss constant, θ (K), of −41 K, which is slightly more negative than that obtained for other 3D Mn−oxalate networks in the $[M^{II}(bpy)_3][Mn_2(ox)_3]$ compounds.[11b,24] These results confirm

(33) Maeda, Y.; Oshio, H.; Tanigawa, Y.; Oniki, T.; Takashima, Y. *Bull. Chem. Soc. Jpn.* **1991**, *64*, 1522.

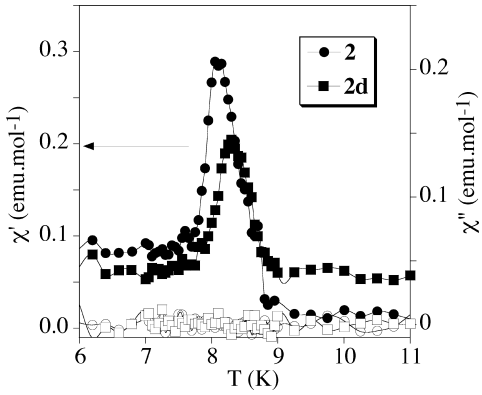

Figure 9. Temperature dependence of the in-phase AC susceptibility (χ'; filled symbols) and the out-of-phase AC susceptibility (χ''; empty symbols) at 1 Hz for **2** (circles) and **2d** (squares).

the antiferromagnetic interaction between Mn(II) ions of the oxalate network and the weak ferromagnet behavior already observed in **1**.

AC susceptibility measurements show a sharp frequency-independent maximum of χ' at 8.1 K (Figure 9) as in that of **1**, but contrary to this compound, no χ'' signal is detected. The position of this maximum in χ' lies between that obtained for **1** (8.0 K) and that for **1d** (8.5 K). The isothermal magnetization at 2 K is very similar to that obtained for **1** and **1d** (see Supporting Information). It presents a hysteresis loop of the magnetization with a coercive field of 66 mT. These measurements indicate that, although no out-of-phase AC signal is detected for **2**, it also presents a magnetic ordering of the oxalate network due to spin canting. The differences between the magnetic behavior of **2** and **1** can be explained by the different angles and distances between Mn(II) ions and by the presence of Fe impurities into the oxalate network of **1** detected by Mössbauer spectroscopy.

The magnetic properties of the desolvated **2** (**2d**) are shown in Figure 8. They are very close to those of the initial compound. As observed for **1**, there is an increase of the temperature of the maximum of χ' from 8.1 to 8.3 K after desolvation (Figure 9). This increase is not as important as for compound **1**, but it presents the same tendency. This could indicate that the structural changes in the anionic network after desolvation can induce the increase of the ordering temperature already observed for the Fe(III) derivative, **1**. The fact that this effect is more important in **1** could indicate that the change of the spin state of the intercalated cation after desolvation also contributes to this effect. A comparative structural study at different temperatures should be performed to clarify this point.

Finally, a preliminary study of the magnetic properties of **1** under light irradiation at 10 K has been carried out. Unfortunately, the magnetization of the compound remains almost unchanged after light irradiation, as expected for this type of compound.[34]

(34) van Koningsbruggen, P. J.; Maeda, Y.; Oshio, H. Iron(III) spin crossover compounds. *Spin Crossover in Transition Metal Compounds I, Topics in Current Chemistry*; Springer: New York, 2004; Vol. 233, pp 259−324.

Conclusion

In this article, we have shown that it is possible to insert the spin-crossover complex $[Fe(sal_2trien)]^+$ into a two-dimensional oxalate-based network of magnetic ions in the compound of formula $[Fe(sal_2trien)]_2[Mn_2(ox)_3]\cdot 4H_2O\cdot C_3H_7NO$ (**1**). We have obtained for the first time a homometallic 2D honeycomb oxalate network formed by magnetic ions. The $[Fe(sal_2trien)]^+$ complexes, which are intercalated between this oxalate's anionic layers, are forming a double layer and lead to a large separation between the anionic layers (17.489(7) Å). The magnetic properties of **1** indicate the coexistence of a magnetic ordering of the Mn(II) oxalate network, which behaves as a weak ferromagnet, and a gradual spin-crossover of half of the intercalated $[Fe(sal_2trien)]^+$ complexes. The most interesting feature of this compound comes from its hybrid character, which allows a combination, in the same compound, of the spin crossover of $[Fe(sal_2trien)]^+$ complexes with the magnetic ordering of an oxalate-based network. A very promising possibility provided by this hybrid strategy is to tune the magnetic ordering of the Mn−oxalate network, inducing the spin-crossover of the intercalated spin-crossover cations by applying light or pressure. In other words, and once it has been shown that hybrid magnets with a coexistence of magnetic ordering and spin-crossover can be designed using a molecular approach, the final goal is to obtain hybrid switchable magnets taking advantage of the switching properties of the spin-crossover network. This goal remains a challenge that has not been reached. Still, the results obtained in this paper constitute an important step in this direction. The insertion of Fe(II) complexes into 3D oxalate-based networks seems to be a better strategy for reaching this goal for several reasons. On the one hand, the changes in geometry of the inserted complex after spin conversion are more important for Fe(II) complexes. On the other hand, and in contrast to Fe(III) complexes, there are many examples of Fe(II) complexes in which spin-crossover can be induced by light or pressure. Finally, the magnetic properties of 3D oxalate networks are very sensitive to the changes of size of the intercalated cation.[11f]

Acknowledgment. Financial support from the European Union (NoE MAGMANet, MERG-CT-2004-508033), the Spanish Ministerio de Educación y Ciencia (Project Consolider-Ingenio in Molecular Nanoscience, CSD2007-00010, and projects CTQ2005-09385-C03 and MAT2007-61584), and the Generalitat Valenciana are gratefully acknowledged. The authors also thank J. M. Martínez-Agudo and Prof. C. J. Gómez-García, University of Valencia, for assistance with the magnetic characterization and Prof. J. F. Létard and Dr. C. Desplanches, ICMCB, CNRS, Université Bordeaux 1, for the magnetic characterization under light irradiation.

Supporting Information Available: Additional figures and a CIF file. This material is available free of charge via the Internet at http://pubs.acs.org.

IC801165B